INTERNATIONAL JOURNAL OF INTEGRATED ENGINEERING
ISSN: 2229-838X e-ISSN: 2600-7916

IJIE

Vol. 17 No. 6 (2025) 40-57
https://publisher.uthm.edu.my/ojs/index.php/ijie

Performance Evaluation of RF Terminators in Butler Matrix System at 28 GHz

Noorlindawaty Md Jizat[1]*, Ayuni Afiqah[2], Norsiha Zainuddin[2], Norazah Abdullah[2], Yoshihide Yamada[2]*

[1] *Centre of Wireless Technology, Faculty of Artificial Intelligence & Engineering, Multimedia University, Cyberjaya, 62300, MALAYSIA*
[2] *Communication Systems and Network (CSN i-Kohza), Malaysia-Japan International Institute of Technology, UTM KL, 54100, MALAYSIA*

*Corresponding Author: noorlindawaty.jizat@mmu.edu.my, yoshihide@utm.my
DOI: https://doi.org/10.30880/ijie.2025.17.06.004

Article Info

Received: 21 March 2025
Accepted: 23 October 2025
Available online: 30 December 2025

Keywords

RF terminator, beamforming, Butler Matrix, signal integrity, loss

Abstract

In wireless network systems, the advancement of wireless technology has made high-frequency systems and beamforming increasingly important with requirement of efficient signal transmission, minimizing crosstalk, and maintain overall system stability. However, these systems are often susceptible to external interference from nearby devices, leading to unwanted signals that interrupt measurement precision and contribute to additional signal losses. Such interference is inevitable due to the sensitivity of the signals. To mitigate the effect, researchers have used metamaterial absorbers, beamforming enhancement, interference cancellation, and cognitive radio techniques. Despite the use of advanced techniques, metamaterials often suffer from resonance-induced reflections. These issues become more pronounced when managing multiple signal paths. In this context, Radio Frequency (RF) terminators play a crucial role in addressing these problems by effectively preventing signal reflections and minimizing transmission losses. In general, systems designed with 50 Ω or 75 Ω terminators experience lower signal losses and improved stability. This paper studies the effect of RF terminators on the performance of a beamforming Butler Matrix, focusing on key elements of current distribution, S-parameters, and output phase. The simulation and measurement results show stable and consistent outputs, with less ripple or distortion when the terminator is applied. The measurement of branch-line coupler indicates a return loss, S_{11} of -17.9 dB, implying minimal signal reflection while the insertion loss, S_{21} and coupling, S_{31} of -3 ± 1 dB, indicates that half of the power is transmitted and equally coupled to the output and the isolation. In addition, S_{41} is -18 dB, confirming good isolation between output ports. The measured return loss of the Butler Matrix is below -10 dB, showing minimal signal reflection, while the transmission amplitude is 6 ± 3.1 dB, reflecting stable signal transmission with small variation. Isolation between ports ranges from -14 dB to -32.2 dB, providing excellent isolation. The output phase has an average deviation of ±10°, ensuring consistent phase performance, highlighting the importance of RF terminators for future research in wireless communication.

1. Introduction

At high frequency, maintaining signal integrity and minimizing losses is critical for reliable performance. This challenge becomes even more significant in beamforming networks, especially in complex multi-port systems [1]. This challenge is not limited to wireless communication; it also extends to other applications such as radar [2], satellite systems, biomedical imaging [3], and automotive sensing, where accurate beamforming, low signal reflection, and reliable system performance are essential to mitigate the adverse effect of high frequency signal degradation. At high frequency, these systems are often susceptible to exterior interference from nearby devices due to the inherent sensitivity of the nature [4]. Recent studies proposed absorptive material of metamaterial[5], enhancing beamforming algorithm[6], interference cancellation technique[7] and cognitive radio [8] to mitigate the interference effect. However, interference mitigation techniques face issues like incomplete cancellation, channel sensitivity, and high complexity, making proper termination the most reliable method to prevent signal degradation from reflections [9], mutual coupling, insertion loss, and impedance mismatches[10].

The role of terminators in improving measurement accuracy, ensuring system stability, and enabling reliable performance is necessary. For instance, Bae et al. [11] emphasize on the significance of precise load termination in multi-port measurements. while Wu et al.[12] discuss how proper termination ensures system stability in oscillatory systems. Bunea et al. [13] highlight the importance of terminators for reliable extraction of parameters in SAW diplexers while in [14], the researchers note that terminators minimize reflections in RF testing setups, and in [15] show that terminators ensure accurate measurements in PCB shielding tests. Ushijima et al. [16] focus on K-band waveguide terminators for precise microwave measurements, and Laur et al. [17] emphasize the need for compact, efficient terminators to maintain signal integrity. A 28 GHz switched-beam antenna system with an integrated Butler Matrix and RF switch was demonstrated in [18], while another design achieved four directional beams with high efficiency and gain using a compact 4×4 Butler Matrix by assuming matched terminations on unused ports [19].

Methodologies for characterizing n-port networks using m-port measurement is explored in [20], emphasizing the importance of terminating unused ports to ensure accuracy in measurements. Recent works reinforce the necessity of proper termination for beamforming integrity [21]. In addition, [22] demonstrated that accurate termination is critical for minimizing return loss and phase errors in 28 GHz phased array systems. The research in [23] also reveals that unterminated ports cause signal distortion in wideband beamforming systems. Additionally, [24] reported that improper port termination leads to amplitude and phase imbalance, compromising beam steering accuracy. Keysight Technologies [25] similarly highlights that reflections from open ports distort S-parameter and return loss measurements. These studies collectively emphasize that RF terminators are vital for achieving high-performance, accurate beamforming. While fundamental simulations have been presented, a comprehensive performance evaluation of the complex multi-port systems such as Butler Matrix incorporating terminators is still lacking.

Driven by this gap, the present study aims to thoroughly investigate how RF terminators influence the performance of a 28 GHz Butler Matrix beamforming network. The research is driven by the need to enhance signal quality, minimize reflections, and improve impedance matching in beamforming systems. The study investigates key performance parameters such as current distribution, S-parameters, and output phase under terminated and unterminated conditions. The analysis is conducted using Computer Simulation Technology (CST) and validated using developed prototype. The results show that proper termination leads to significantly improved performance, including ripple-free outputs, better signal balance, and more accurate phase alignment. This study emphasizes the important role of RF terminators in multi-port networks and highlights the importance of optimizing beamforming systems, particularly in next-generation 5G and high-frequency applications.

2. Simulation Results

The simulation was performed using CST software to investigate the design structure of the Butler Matrix with and without terminator. The performance for each stage of the Butler Matrix elements was thoroughly analyzed.

2.1 Branch-line Coupler Elements

The coupler structure consists of four ports, with the input signal fed to any of the ports. As shown in Fig. 1, the input is applied to Port 1 (P1) and Port 2 (P2), while Ports 3 (P3) and 4 (P4) are the output and isolation ports, respectively. The feed width, W_f, is calculated based on an impedance of $Z_0 = 50\ \Omega$ and an electrical length of $\lambda/4$. The widths W_z and W_{z0} are determined using the impedances Z_0 of 50 Ω and Z_1 of 35.35 Ω. The detailed dimensions are summarized in Table 1. In the simulation, the designated port is fed with the input signal, while the other ports are connected to terminators. The termination is modeled in CST using a 50-ohm resistor, ensuring matched impedance and the electric field boundary is set to $E_t = 0$. In two port measurement of S_{21} , the signal is applied to P1 and P2, and while P3 and P4 are terminated. The material used is from Nippon Pillar Packing Co.,

Int. Journal of Integrated Engineering Vol. 17 No. 6 (2025) p. 40-57

Ltd. where the height is 0.254 mm, permittivity is 2.2, and a tangent loss is 0.0007. The material has low dielectric loss and has stable dielectric properties.

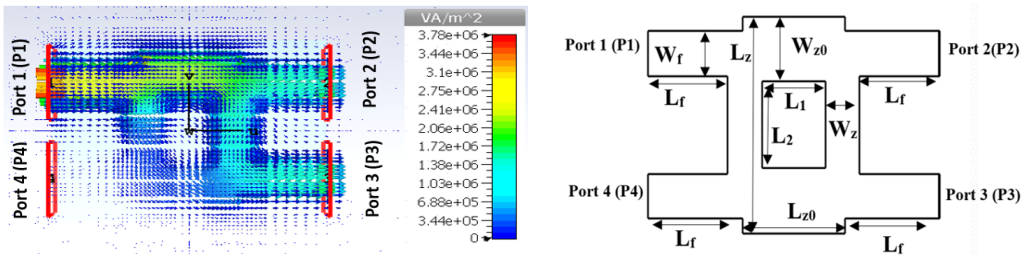

(a) **(b)**

Fig. 1 *The coupler (a) design; and (b) dimensions*

Table 1 *Parameter of the branch-line coupler structure*

Parameter	Value	Parameter	Value
W_f	0.84	L_z	3.74
W_{zo}	0.971	L_1	1.2
W_z	0.76	L_2	1.8
L_{zo}	2.11	L_f	2.5

To achieve impedance matching, the characteristic impedance Z_1 should be calculated as $Z_1 = \sqrt{R_{in}Z_0}$, where Z_0 represent the real impedance. The reflection, r(x), representing the S-parameter is determined by the following Equation (1)[26]:

$$r(x) = \frac{v^-(x)}{v^+(x)} = r(0) = \frac{Z_L - Z_0}{Z_L + Z_0} \quad (1)$$

with v^+ denote forward signal and v^- denote reverse signal.

The current distribution without the terminator is shown in Fig. 2, while the performance with the terminator is shown in Fig. 3. The branch-line coupler produces a signal that is uniformly distributed between output ports 2 (P2) and port 3 (P3), as the structure provides a −3 dB coupling. From the configurations, no return wave is observed; nonetheless, the power density shows that the design with the terminator produces equal signal flow.

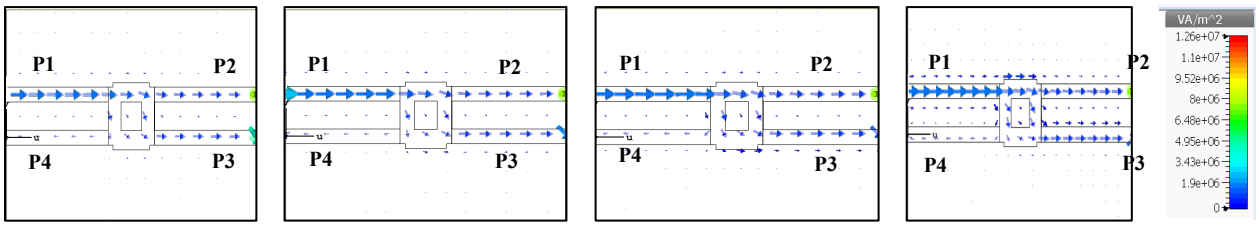

(a) **(b)** **(c)** **(d)**

Fig. 2 *Current distribution of coupler with a termination load when fed at P1 (a) 90°; (b) 180°; (c) 270°; and (d) 360°*

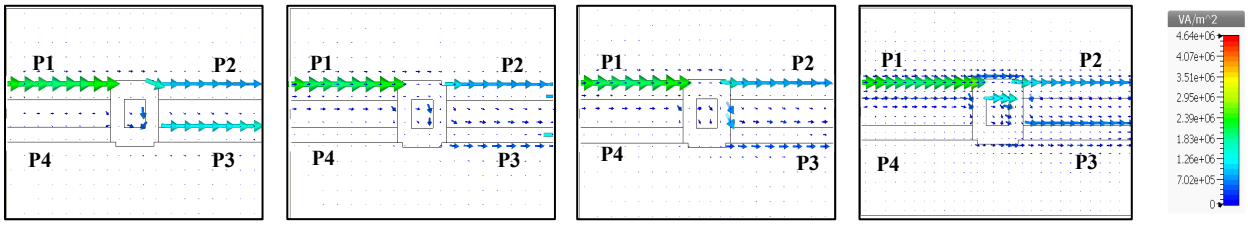

Fig. 3 *Current distribution of coupler without a termination load when fed at P1 (a) 90°; (b) 180°; (c) 270°; and (d) 360°*

Branch-line coupler design's performance has been investigated using the information obtained from Fig. 4 for return loss, S_{11}, insertion loss, S_{21}, coupling, S_{31}, isolation, S_{41}, and output phase. In the absence of the terminator, S_{11}, S_{21}, S_{31} and S_{41} have respective values of -19.3 dB, -5 dB, -2.18 dB, and -25.5 dB. After applying the terminator, these values change to -3.1 dB, -3.9 dB, -11.55 dB, and -21.18 dB. Connecting the terminator results in a consistent and steady signal distribution in the simulation. This results from the termination's impedance matching with the output port's transmission line, which removes signal reflections and guarantees signal stability. In contrast to the design without the terminator, the return loss for the terminator-equipped design shifts to a lower frequency. According to Fig. 5, the output phase simulation indicates that $\angle S_{21}$ and $\angle S_{31}$ are both -85°. Furthermore, the simulation shows that when the terminator is used, the −10 dB fractional bandwidths for the isolation, $|S_{41}|$, and return loss, $|S_{11}|$, are 40.7% and 41%, respectively. The calculation of the −10 dB bandwidth is described in [26], and Equation (2) uses f_0 as the center frequency.

$$BW_{percentage} = \frac{100\Delta f}{f_0} \tag{2}$$

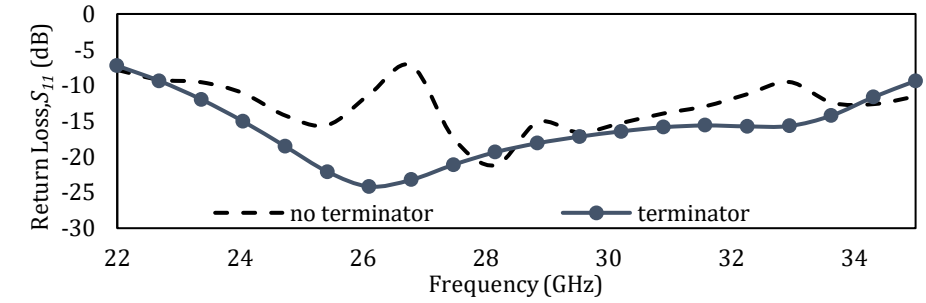

(a)

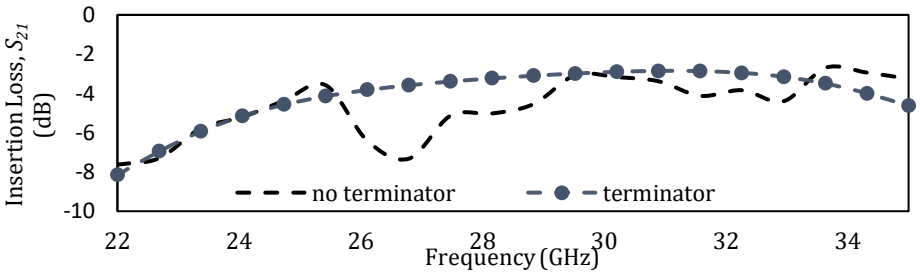

(b)

Int. Journal of Integrated Engineering Vol. 17 No. 6 (2025) p. 40-57

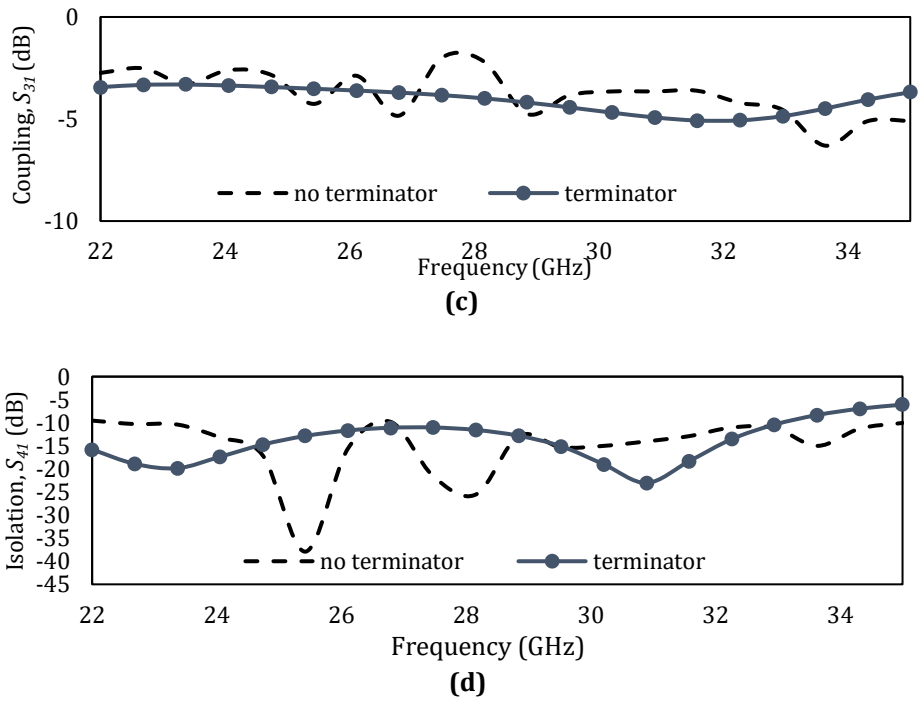

Fig. 4 *S-Parameter analysis with and without termination load of (a) S_{11}; (b) S_{21}; (c) S_{31}; and (d) S_{41}*

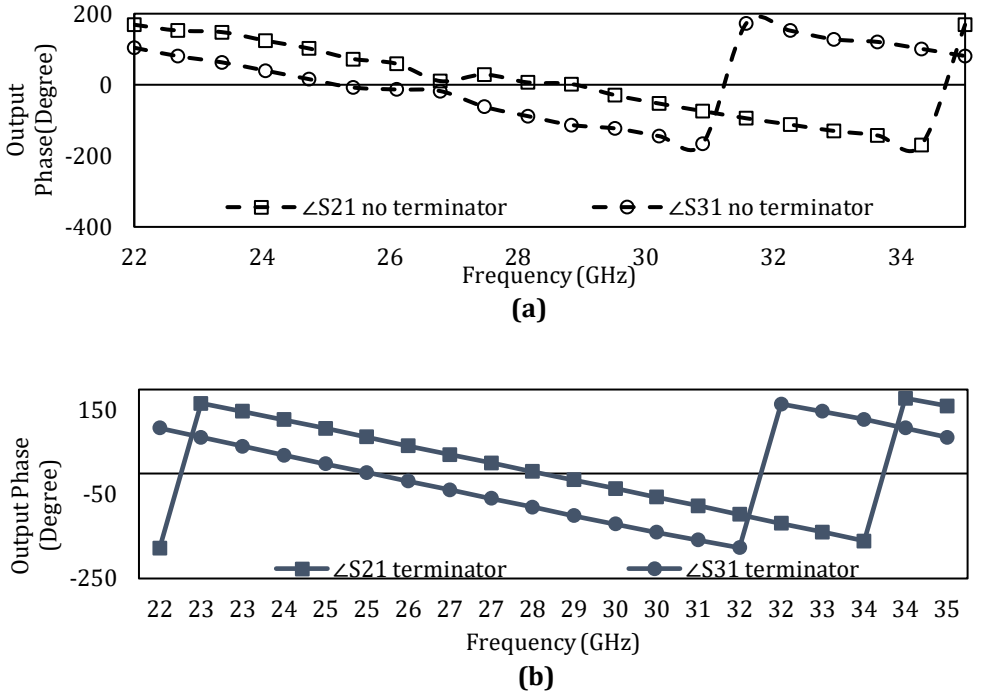

Fig. 5 *Output phase of coupler with (a) no termination load; and (b) with termination load*

2.2 Crossover Elements

Fig. 6 shows the current distribution without the terminator, while Fig. 7 presents the current distribution when the terminator is applied. The crossover is designed to achieve minimal coupling, with S_{31} at 0 dB and the current flows from P1 to P3. In the structure without the terminator, some of the signals are directed to P4 at a 360° input phase. However, when the circuit is connected with the terminator, no reflected power is observed. The return loss, S_{11} and coupling, S_{31}, presented in Fig. 8, are −14.93 dB and −2.2 dB, respectively when ports are connected to the terminator. While the

structure without the terminator shows better values in terms of performance, the simulation shows signal distortion and exhibits ripple.

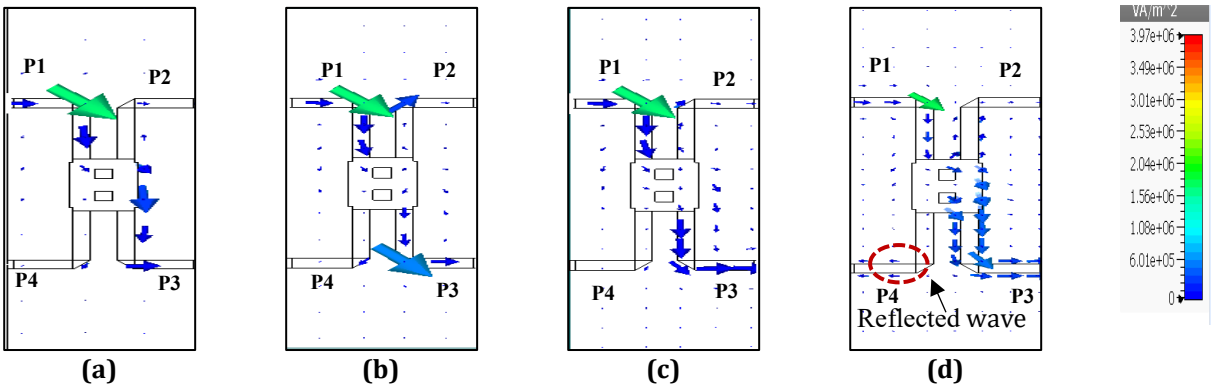

Fig. 6 *Current distribution of crossover without termination load at phase (a) 90°; (b) 180°; (c) 270°; and (d) 360°*

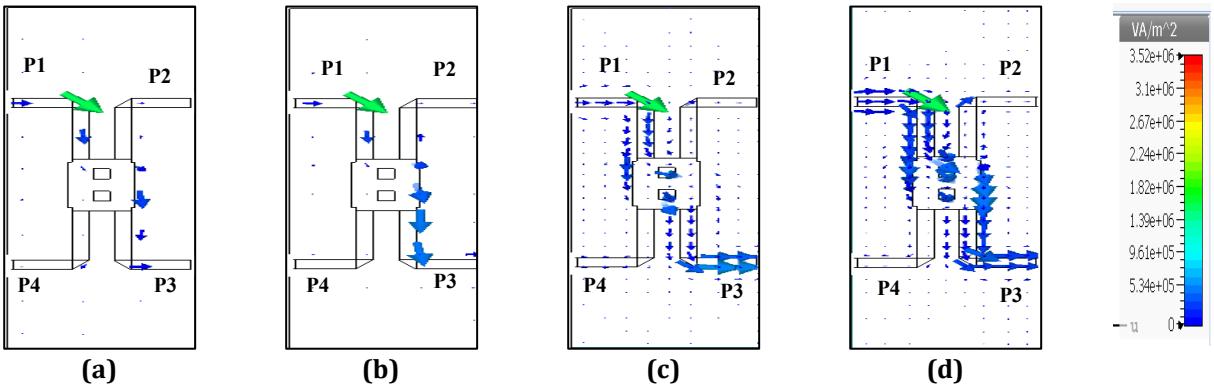

Fig. 7 *Current distribution of crossover with termination load at phase (a) 90°; (b) 180°; (c) 270°; and (d) 360°*

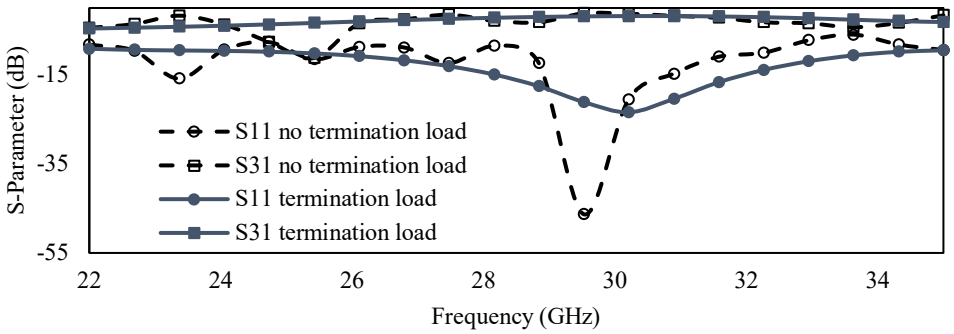

Fig. 8 *S-Parameter for S_{11} and S_{31} with and without the termination load*

2.3 Butler Matrix Elements

The Butler Matrix has branch-line coupler, phase shifters and crossover, where the configuration is shown in Fig.9. The power signal for the structure which is not using terminator is illustrated in Fig. 10 while Fig. 11 shows the power signal when the terminator is applied. Without the terminator, some of the signal reflects to the input port (P4) during 270° and 360° phase. However, the current distribution is uniform and coupled equally at the output port with the usage of the terminator. Fig. 12 to Fig. 19 exhibit the performance when the structure is attached to the terminator and without. Return loss, S_{11} for both configuration shows promising result which is below −10 dB. However, the Butler Matrix without the termination load has ripple and distortion. In the Butler Matrix with the termination load, the bandwidths $|S_{11}|$ is 34.6 %. The transmission amplitude represents the relationship between the output and input power, where theoretical value of −6 dB. The terminated Butler Matrix produces a

Int. Journal of Integrated Engineering Vol. 17 No. 6 (2025) p. 40-57

uniform and equally distributed output signal with the S_{51}, S_{61}, S_{71}, and S_{81} shows the value of −6 ± 4 dB. The output phase with no terminator exhibits ripple and is not recurring. In the Butler Matrix with the termination load, the uniform output phase at 28 GHz with phase difference of ±45± 5° and ±135± 5° is observed.

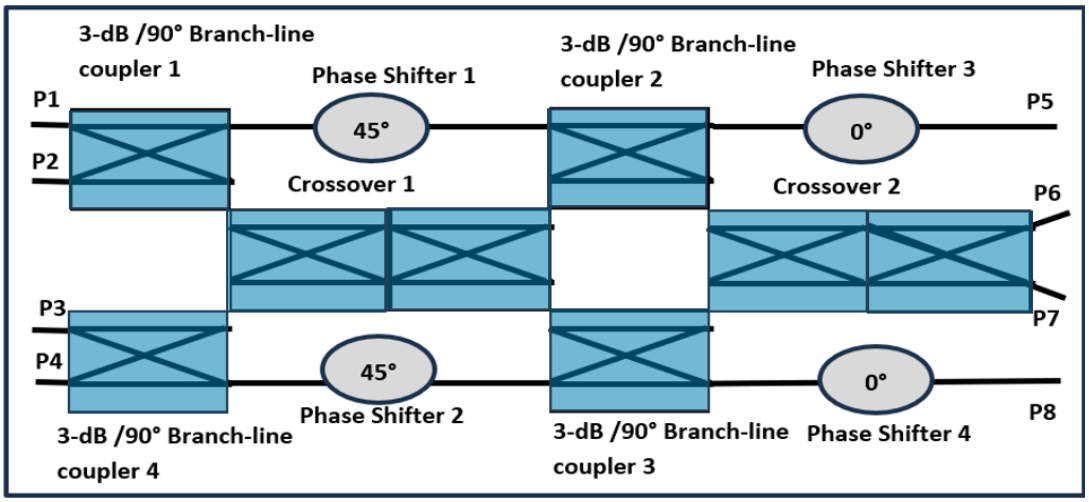

Fig. 9 *Butler Matrix structure with the elements*

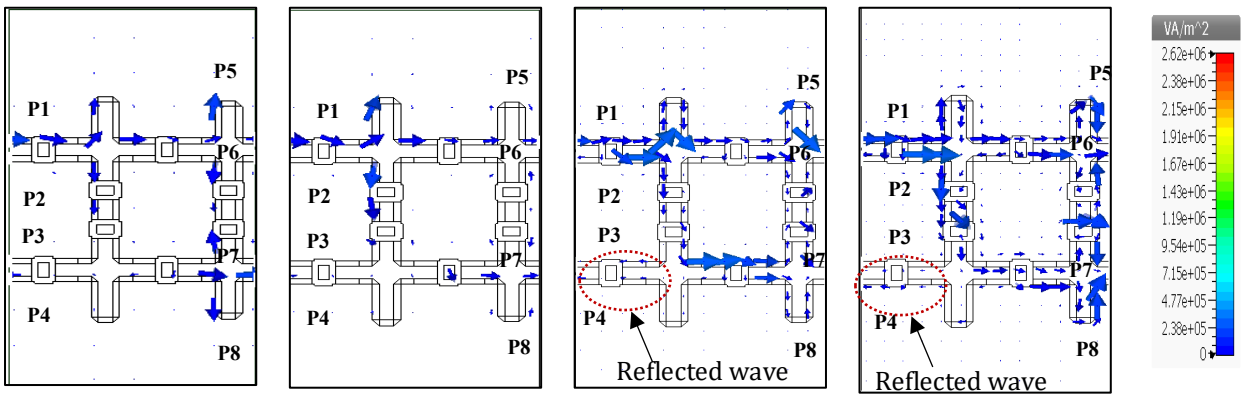

Fig. 10 *Current distribution without termination load at input phase (a) 90°; (b) 180°; (c) 270°; and (d) 360°*

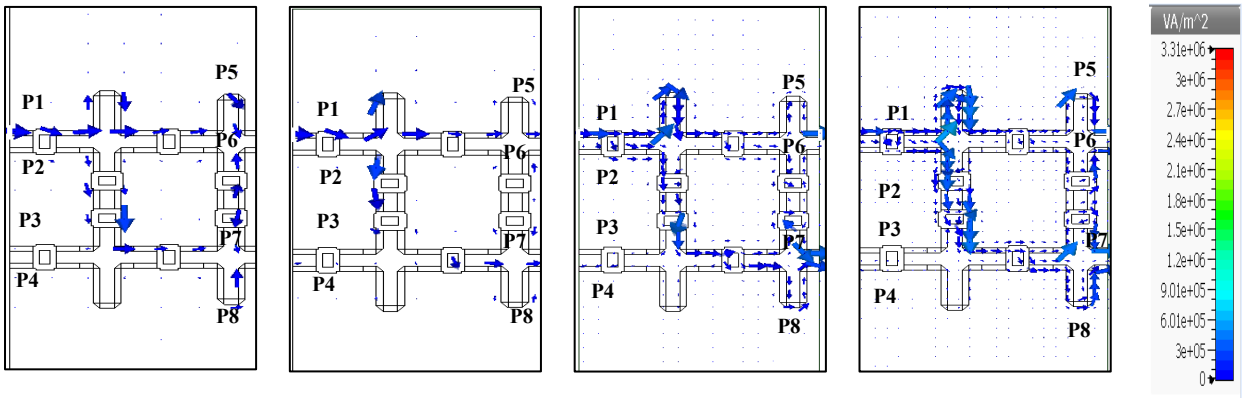

Fig. 11 *Current distribution with termination load at input phase (a) 90°; (b) 180°; (c) 270°; and (d) 360°*

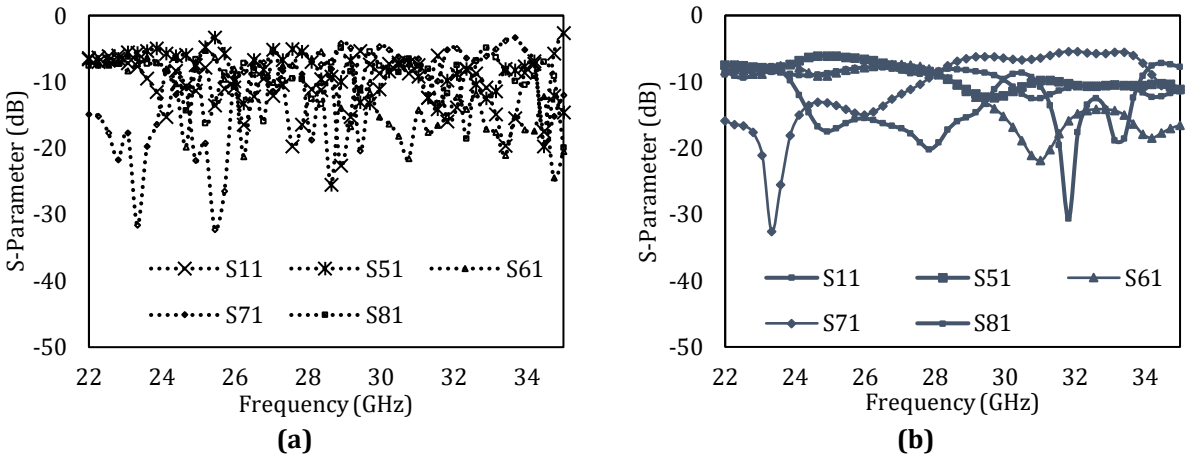

Fig. 12 *S-Parameter at Port 1 (a) without termination load; and (b) with termination load*

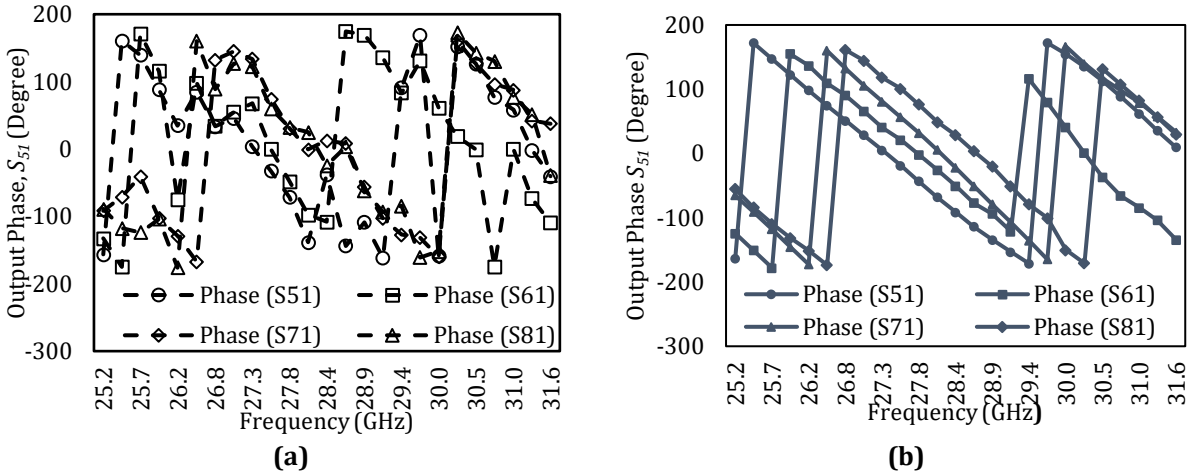

Fig. 13 *Output phase at Port 1 (a) without termination load; and (b) with termination load*

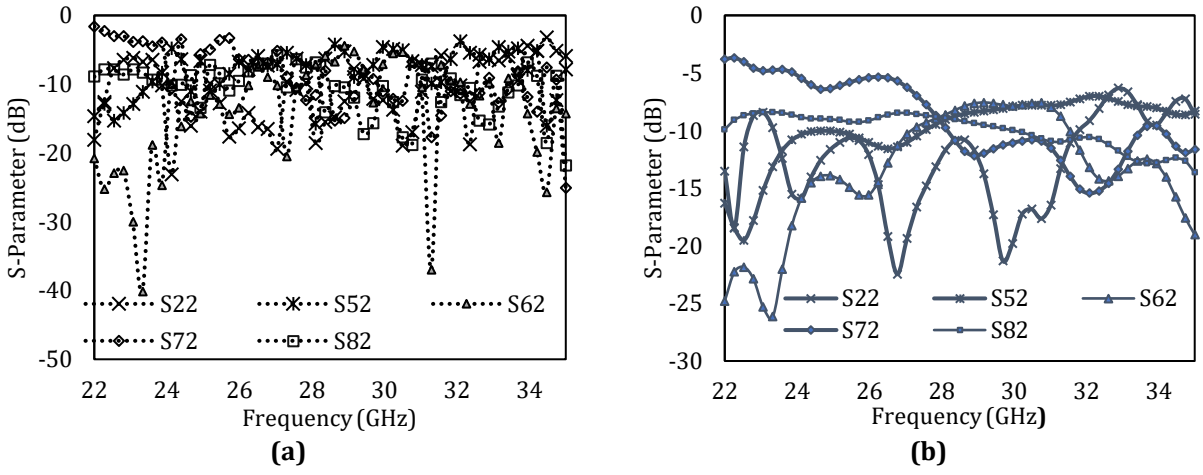

Fig. 14 *S-Parameter at Port 2 (a) without termination load; and (b) with termination load*

Int. Journal of Integrated Engineering Vol. 17 No. 6 (2025) p. 40-57

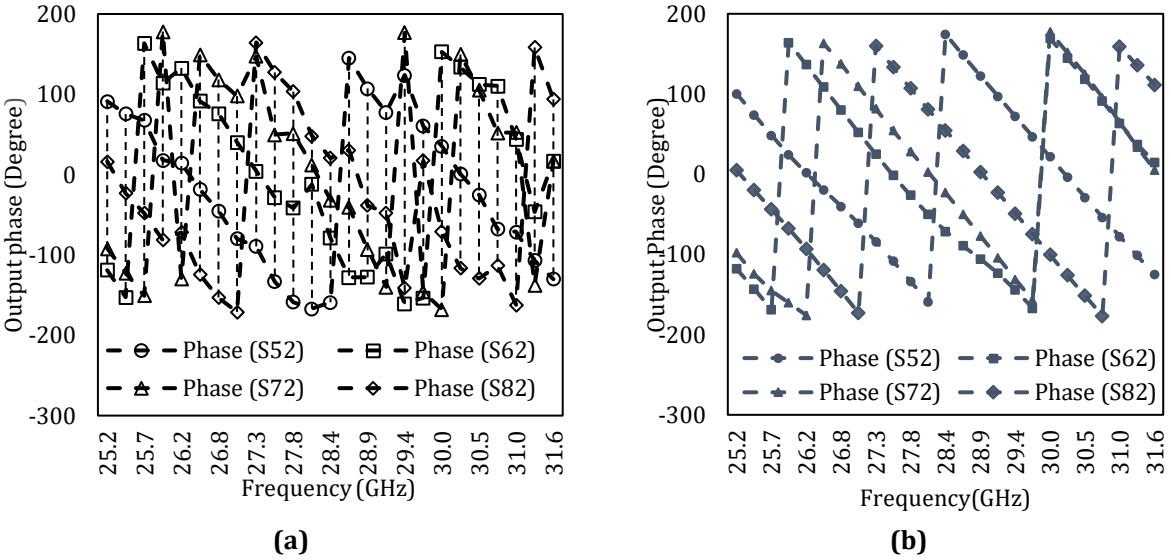

Fig.15 *Butler Matrix output phase at Port 2 (a) without termination load; and (b) with termination load*

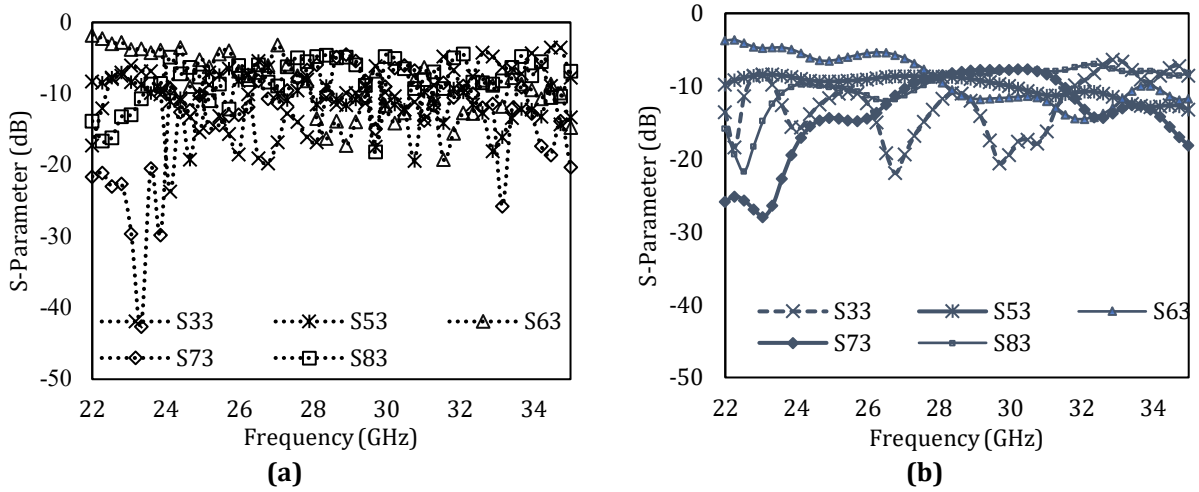

Fig. 16 *S-Parameter at Port 3 (a) without termination load; and (b) with termination load*

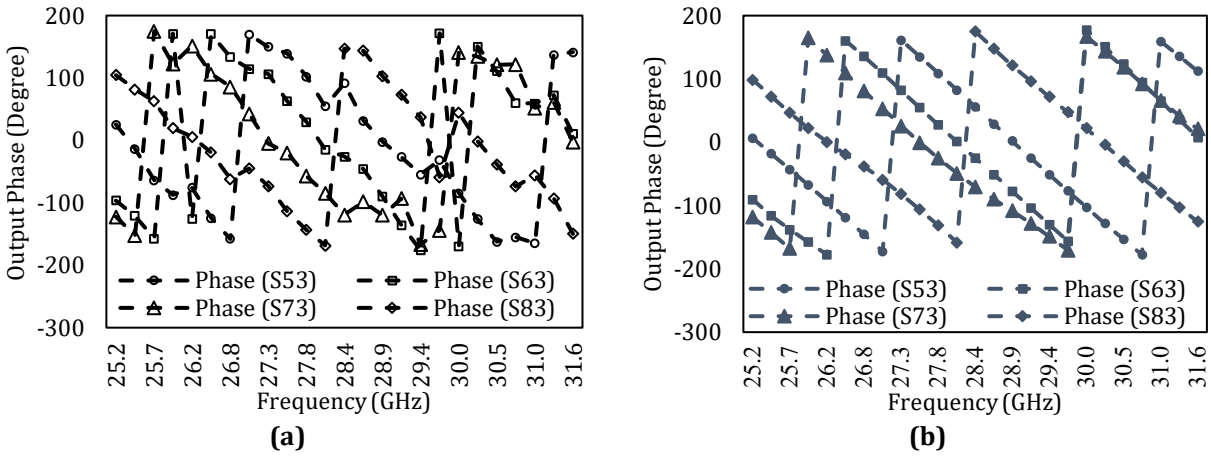

Fig. 17 *Output phase when Port 3 is fed (a) without termination load; and (b) with termination load*

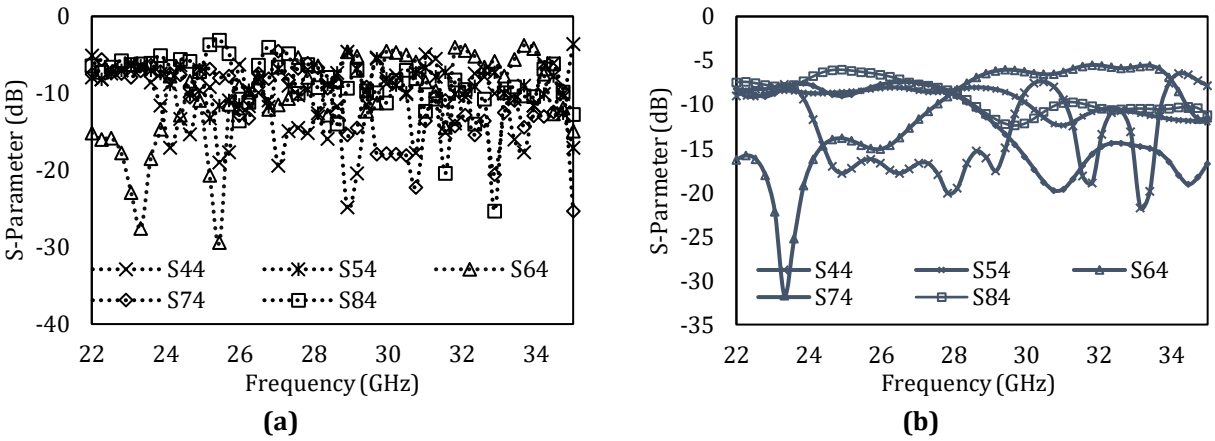

Fig. 18 *S-Parameter at Port 4 (a) without termination load; (b) with termination load*

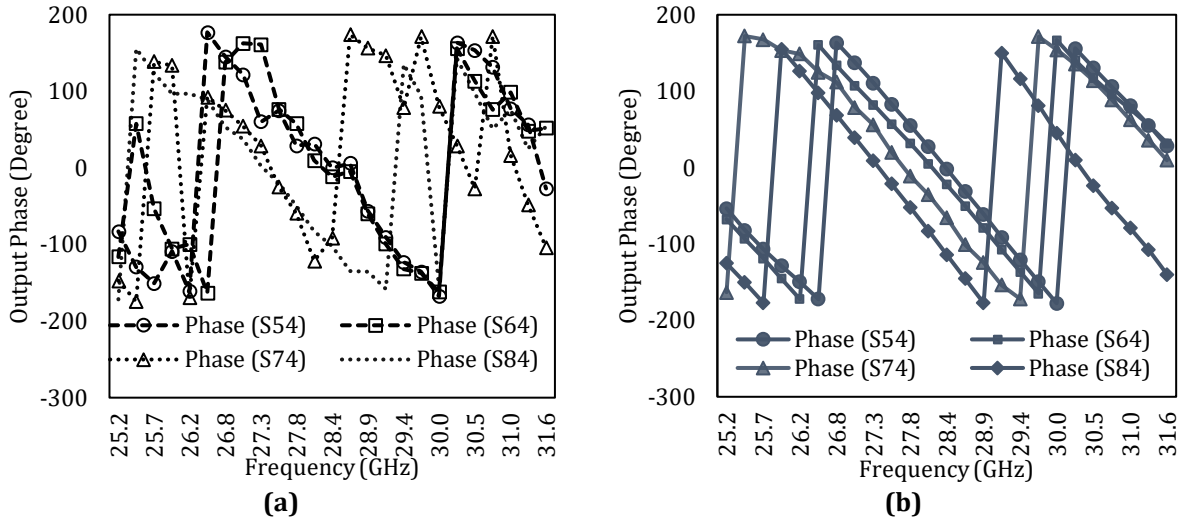

Fig. 19 *Output phase when Port 4 is fed (a) without termination load; and (b) with termination load*

3. Measurement Results

Fig. 20 depicts the VNA connector cable and the measurement for the Butler Matrix. The reflection coefficient is measured using the one-port VNA network, while the transmission coefficient and the phase difference are measured using the two-port VNA network.

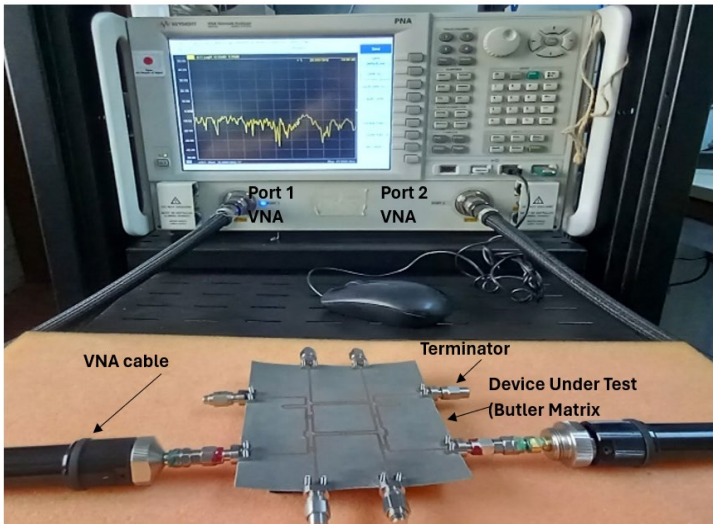

Fig. 20 *VNA connector cable with Butler Matrix*

Int. Journal of Integrated Engineering Vol. 17 No. 6 (2025) p. 40-57

3.1 Branch-line Coupler

The prototype has a dimension of 20 cm ×20 cm in size. Fig. 21 shows the configuration measurement setup for return loss, one port where the VNA cable is connected to port measurement, Port 1 while the unused port is connected to the terminator. The same technique is applied to determine the value of the coupling, S_{21}, S_{31} , isolation, S_{41} and the output phase.

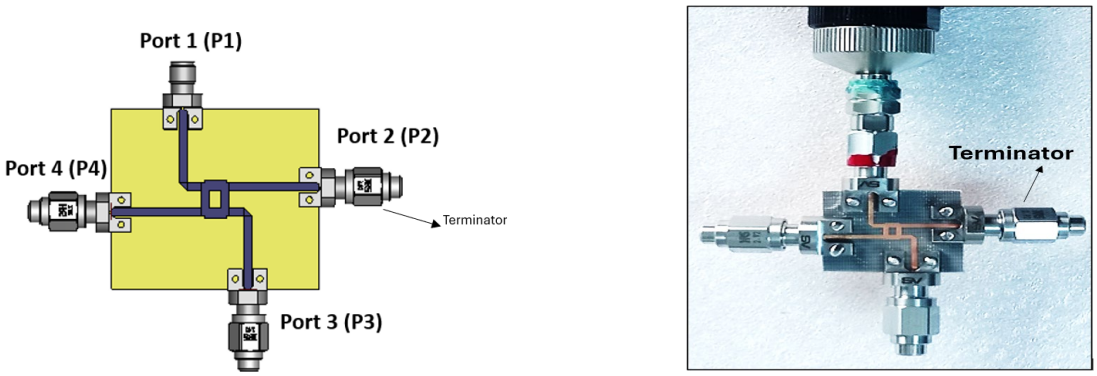

Fig. 21 *Configuration measurement for return loss,* $\boldsymbol{S_{11}}$

As shown in Fig. 22, the simulation return losses at the branch-line coupler at 28 GHz are −20.1 dB, −20.1 dB, −20.55 dB, −20.5 dB while the measurement return loss are −17.9 dB, −17.2 dB, −17.5, and −18 dB for S_{11}, S_{22}, S_{33} and S_{44}, respectively. The simulations are −3.78 dB, -3.8 dB and −23.2 dB while the measurements are −3 dB, −4.34 dB and −18 dB for the insertion loss, S_{21}, coupling, S_{31} and the isolation, S_{41}, respectively. The simulation of the output phase difference is −89°, while the measurement is −88°. The simulation of bandwidths percentage of |S11| is 36.52% and |S41| is 41% while for the measurement |S11| is 55% and isolation, |S41| is 50%. The bandwidth calculation is obtained in [26] where f_0 is the resonant frequency as expressed in Equation (3):

$$BW_{percentage} = \frac{100\Delta f}{f_0} \tag{3}$$

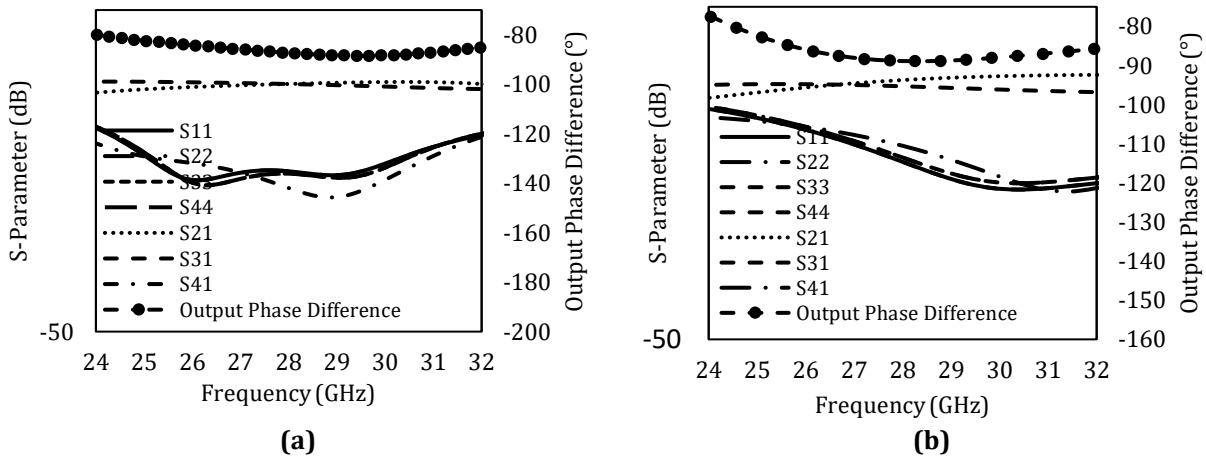

Fig. 22 *Branch-line coupler* $S_{11}, S_{22}, S_{33}, S_{44}, S_{21}, S_{31}, S_{41}$ *and the output phase (a) simulation; and (b) measurement*

3.2 Butler Matrix

In the measurement methodology, calibration is performed using short, open, load and through Vector Network Analyzer (VNA) kit to ensure accuracy. For Butler Matrix, both one-port and two-port configurations are as illustrated in Fig. 23 and Fig. 24. The one-port setup is utilized for return loss, S_{ii} measurements with i represent the input and output ports. The VNA is connected to a specific input port while all unused ports (P2–P8) were

terminated with matched loads to maintain uniform test conditions. Two-port measurements are used to find the transmission amplitudes, output phase and isolation. The VNA is connected to two corresponding ports while the remaining ports were properly terminated. These configurations are maintained throughout the testing to ensure a uniform application method and minimize variability. This study distinctively integrates RF terminators into the Butler Matrix, developing signal integrity and beamforming precision with potential applications extending to radar systems, satellite communications, biomedical imaging, and IoT technologies.

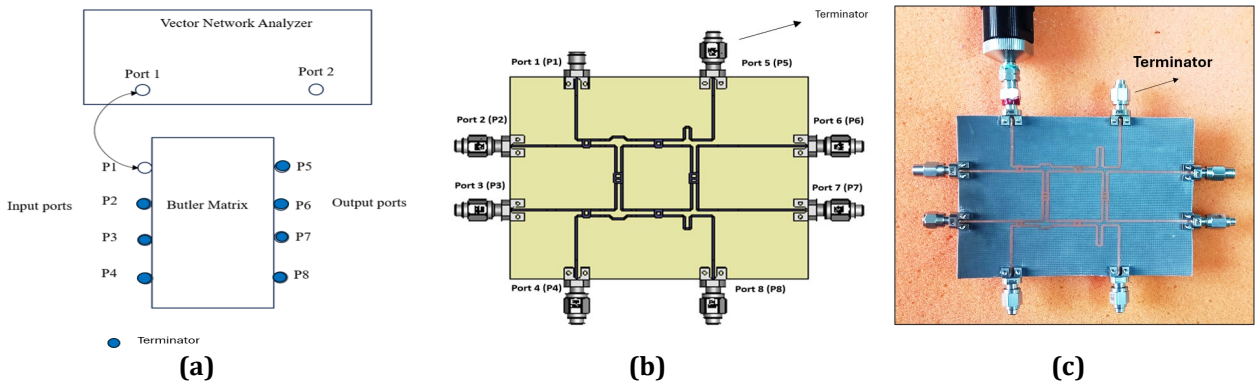

(a) **(b)** **(c)**

Fig. 23 *Configuration of one-port Butler Matrix with terminator (a) diagram; (b) simulation; (c) fabricated model*

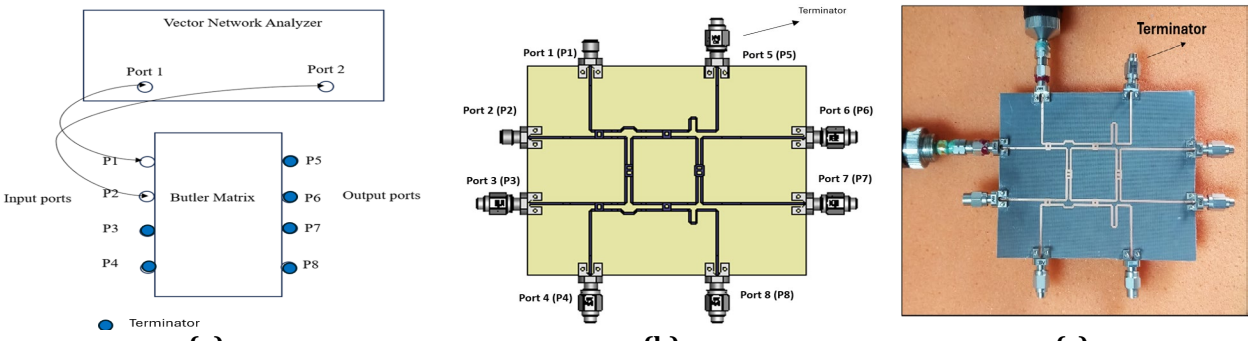

(a) **(b)** **(c)**

Fig. 24 *Configuration of two-port Butler Matrix with terminator (a) diagram; (b) simulation; (c) fabricated model*

3.2.1 Impedance measurement

The impedance measurements of the Butler Matrix are tested with and without the terminator. After calibration is completed, the Butler Matrix under test is connected to VNA, while all remaining ports are left terminated and unterminated accordingly, allowing for comparative testing of impedance value under separate loading. Fig. 25 shows the measurement value for the line impedance for the configuration with and without the terminator using VNA. The configurations with terminator provide the impedance, Z of 49 Ω while the configuration without the terminator provide the value of impedance, Z of 40 Ω. The corresponding impedance between the input and the output port can be observed when the terminator is fed to the port. For $Z = Z_0$, the impedance matching is at the centre of the Smith Chart, or the total of the impedance calculated is 50 Ω from Equation (4) indicating R is the resistance value and X_L is the reactance value:

$$Z = \sqrt{R^2 + {X_L}^2} \tag{4}$$

Int. Journal of Integrated Engineering Vol. 17 No. 6 (2025) p. 40-57

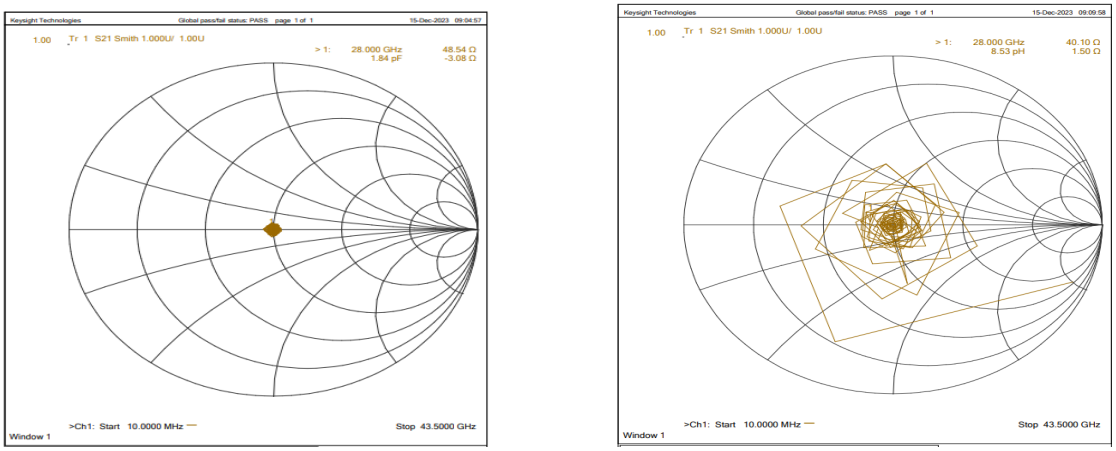

(a) **(b)**

Fig. 25 *Measurement for the line impedance of via-hole (a) with terminator; (b) without terminator*

3.2.2 Return Loss

The return loss of Butler Matrix is illustrated in Fig. 26. As 28 GHz, the input return losses are −27 dB, −24.1 dB, −23 dB, −26 dB, −25.6 dB, −23.1 dB, −24.2 dB, and −26.84 dB for $\boldsymbol{S_{11}}$, $\boldsymbol{S_{22}}$, $\boldsymbol{S_{33}}$, $\boldsymbol{S_{44}}$, $\boldsymbol{S_{55}}$, $\boldsymbol{S_{66}}$, $\boldsymbol{S_{77}}$, and $\boldsymbol{S_{88}}$ respectively. The return losses for $\boldsymbol{S_{11}}$, $\boldsymbol{S_{44}}$, $\boldsymbol{S_{55}}$ and $\boldsymbol{S_{88}}$ are equal at −26.84 dB, while $\boldsymbol{S_{22}}$, $\boldsymbol{S_{33}}$, $\boldsymbol{S_{66}}$, and $\boldsymbol{S_{77}}$ are the same at −23.68 dB. In comparison, the measured value are −19.7 dB, −12.6 dB, −18.1 dB, −19.8 dB, −16.2 dB, −12 dB, −12.6 dB, and −17.4 dB for $\boldsymbol{S_{11}}$, $\boldsymbol{S_{22}}$, $\boldsymbol{S_{33}}$, $\boldsymbol{S_{44}}$, $\boldsymbol{S_{55}}$, $\boldsymbol{S_{66}}$, $\boldsymbol{S_{77}}$, and $\boldsymbol{S_{88}}$, respectively. The simulation results show a −10 dB bandwidth percentage of 46% for $|S_{11}|$ and 45% for $|S_{41}|$, while the measured values are 25.8% for $|S_{11}|$ and 24.6% for $|S_{41}|$. The return losses show the value below −10 dB, which represent effective transmission power.

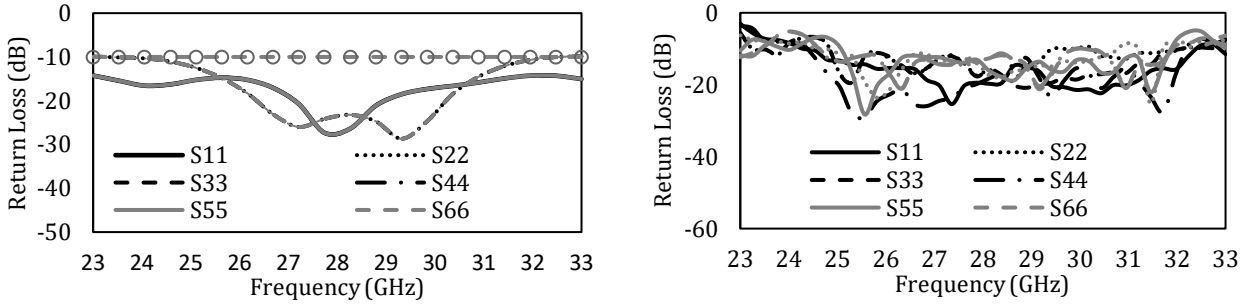

(a) **(b)**

Fig. 26 *Conventional Butler Matrix return losses of the input (a) simulation; and (b) the measurement results*

3.2.3 Transmission Amplitude

Fig. 27 displays the simulated and measured transmission amplitudes. Theoretically, the transmission amplitude is −6 dB when the input is fed. As shown, the simulation of the transmission amplitude at the input 1 at each output are −7.16 dB, −7.1 dB, −7.35 dB, −6.74 dB while the measurements are −9.6 dB, −9.2 dB, −8.52 dB and −9.3 dB for S_{51}, S_{61}, S_{71} and S_{81}. Meanwhile the simulation of the transmission amplitude at the input 2 at each output are −8.1 dB, −8.5 dB, −8.6 dB and −7.3 dB while the measurements are −9.8 dB, −8.6 dB, −8.7 dB and −9.4 dB for S_{52}, S_{62}, S_{72} and S_{82}. The transmission amplitude at the input 3 at each output are −7.3 dB, −8.7 dB, −8.7 dB and −8.1 dB while the measurements are −9 dB, −8.7 dB, −9.5 dB and −9.7 dB for S_{53}, S_{63}, S_{73} and S_{83} while the transmission amplitude at the input 4 at each outputs are −6.9 dB, −7.3 dB, −7 dB, −7.2 dB while the measurements are −9 dB, −8 dB, −9.4 dB and −9 dB for S_{54}, S_{64}, S_{74} and S_{84}, respectively. The average transmission amplitude for the simulation is −7.62 dB and the measurement are −9 dB with the tolerance of −6 ± 3.1 dB.

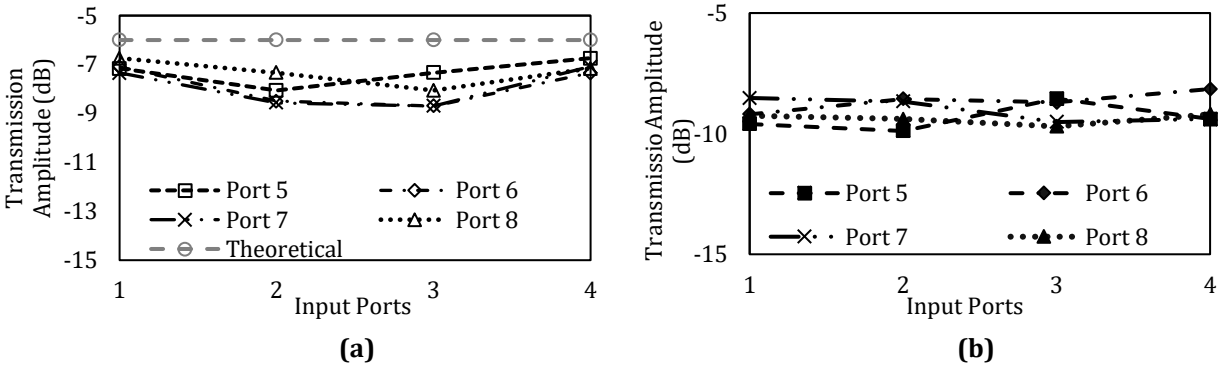

Fig. 27 *Transmission amplitudes (a) simulation; and (b) measurement*

3.2.4 Isolation

The simulation and measurement isolations are shown in Fig. 28 and Fig. 29, with simulated isolations ranging from −20 dB to −42.5 dB and measured isolations ranging from −14 dB to −32.2 dB. Ideally, the isolations are less than −10 dB.

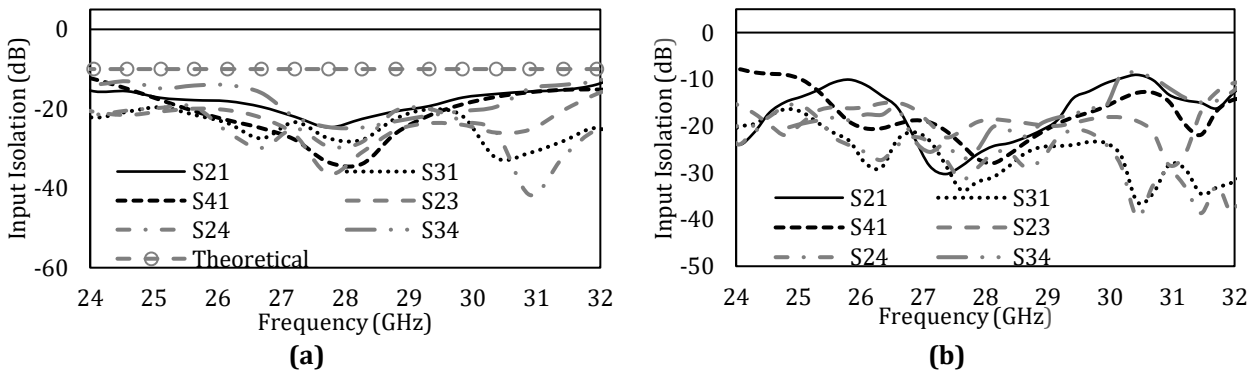

Fig. 28 *Isolation at the input ports (a) simulation results; (b) measurement results*

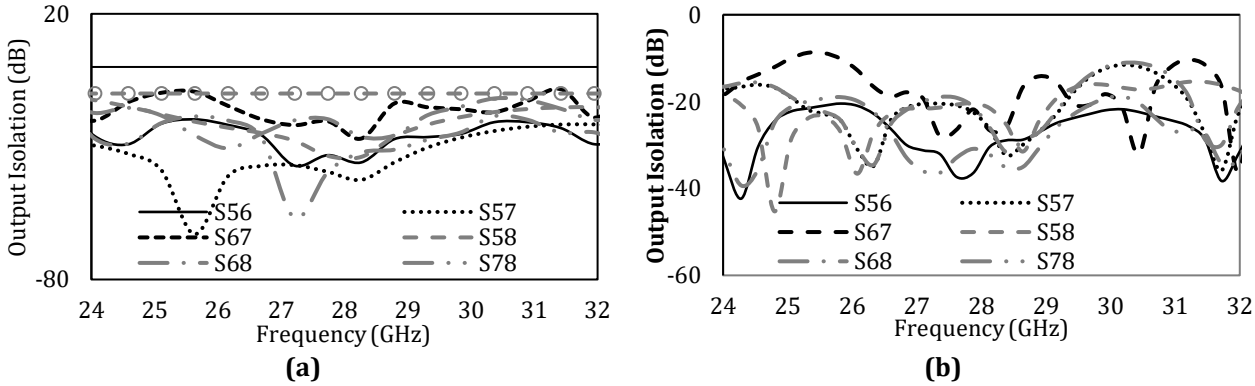

Fig. 29 *Isolation at the output ports (a) simulation results; (b) measurement results*

3.2.5 Output Phase

The output phases are shown in Fig. 30, where the theoretical output phase differences for Port 1 are −45°, Port 2 are +135°, Port 3 are −135° and Port 4 are +45°. For Port 1, the simulation results are 0°, −41°, −84° and −140° while the measurements are 0°, −44°, −92° and −145°. In port 2, the simulation results are 0°, +130.59°, +260.16° and +395.74° while the measurements are 0°, +137°, +280° and +435°. Meanwhile in Port 3, the simulation results are 0°, −132.55°, −270° and −406.66° while the measurements are 0°, −147°, −292° and −463°. For Port 4,

Int. Journal of Integrated Engineering Vol. 17 No. 6 (2025) p. 40-57

the simulation results are 0°, +49.95°, +94° and +139° while the measurements are 0°, +50°, +120° and +155°. From the results obtained, the output phases show constant difference changes. The performances of Butler Matrix are justified by comparing the data result with the theoretical output difference phases. The output phases show a level of consistency, with an average of ±10°. This error is attributed to fabrication tolerance as well as the conventional Butler Matrix components, which require additional transmission lines for the feedlines and the coaxial cable loss.

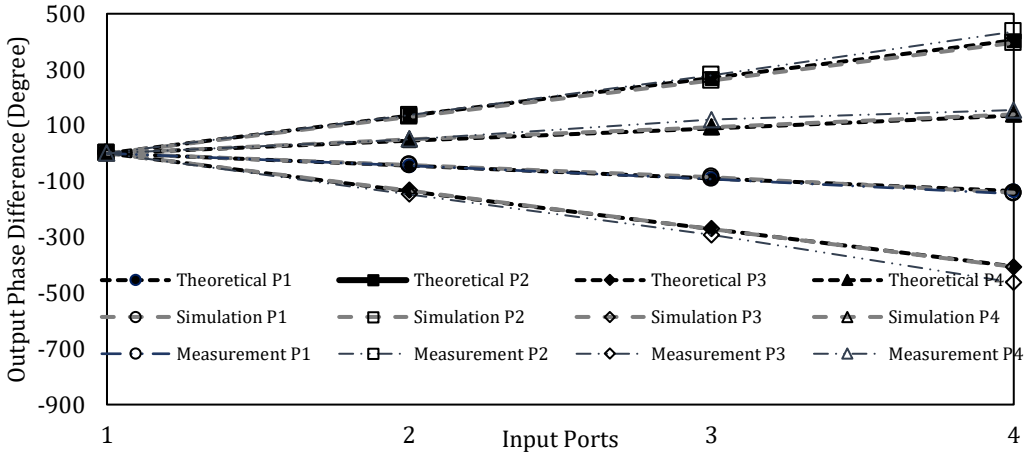

Fig. 30 *Theoretical, simulated and measured of the output phases*

3.2.6 Summary

Table 2 presents a comparison of selected RF system designs with an emphasis on terminator usage. While most studies focus primarily on switching integration, compactness, or mid- to high-frequency operation, they do not explicitly address RF terminator effects. A design of a 4×4 switch-integrated Butler matrix is discussed in [18], at the same frequency but do not address termination, focusing instead on switch behavior. Similarly, [27] develop a beam-switching system with integrated antennas and a Butler matrix at 28 GHz, though terminators are not considered in their design. In [28], the researchers propose a 5×5 matrix for 3.3–3.7 GHz operation, emphasizing gain and efficiency, again without terminator evaluation. A standalone termination design is discussed in [9], though it is not embedded within a full matrix system. Lastly, [29] introduce a compact SICL-based 4×4 Butler Matrix operating at 56–68 GHz, prioritizing miniaturization over termination effects. In contrast, this paper incorporates and analyzes RF terminators directly in a 28 GHz Butler matrix configuration, offering insights into their influence on return loss, phase consistency, and insertion loss. This contributes to a broader understanding of terminator roles in high-frequency beamforming systems. This paper fills a critical gap by providing empirical analysis of terminators within the complete Butler matrix system, offering insights not addressed in prior research. These improvements have potential relevance for various high-frequency applications, including satellite communications, automotive radar, biomedical implants, industrial IoT, and high-speed data transmission, where managing interference and maintaining system reliability are important considerations.

Table 2 *Comparison of RF system designs with focus on terminator usage*

References	Terminator studied?	Frequency Band	Key findings	Remarks
[18]	Not discussed	28 GHz	Switch-integrated Butler matrix with 4×4 design	No terminator consideration, switch performance emphasized
[27]	Not discussed	28 GHz	Beam switching with integrated antenna array	Antenna + matrix focus; terminators assumed ideal
[28]	Not discussed	3.3–3.7 GHz	5×5 Butler matrix, beam gain ~11.4 dBi, efficiency ~83.8%	Mid-band, no terminator evaluation

References	Terminator studied?	Frequency Band	Key findings	Remarks
[9]	Standalone terminator proposed	20–67 GHz	Microstrip-based termination load with absorber; RL < –10 dB	Not integrated in Butler matrix; potential for future use
[29]	Not discussed	56–68 GHz	SICL-based 4×4 Butler matrix, compact ultra-wideband design	Focus on compact implementation; no port termination analysis
This paper	Explicit analysis of RF terminator	28 GHz	Improved return loss (< –10 dB), balanced phase, low insertion loss	Focus on practical impact of terminator in full system

4. Conclusion

This study presents a comprehensive investigation into the role of RF terminators in enhancing the performance of a Butler Matrix beamforming network. In the first part of the discussion, simulations of the branch-line coupler, the crossover and the Butler Matrix are performed using CST by analyzing key parameters including current distribution, S-parameters, and output phases with and without the 50-ohm terminator. The results show that when unused ports are terminated with matched loads, current is distributed more evenly across the network components, reducing reflections and losses. Specifically, properly terminated configurations exhibit balanced and ripple-free signal transmission, especially in critical elements like the crossover, where the current flow in forward direction and no reflection is observed. In contrast, unterminated configuration suffers from signal reflections and impedance mismatches that degrade performance. The second part discusses the simulation and measurement results of the terminated Butler Matrix. The analysis includes impedance, branch-line couplers, S-Parameter and output phase of the Butler Matrix. The measurement results show good agreement with the simulation results. The impedance measurement showing the matched impedance when connected to the terminator. The branch-line coupler also shows comparable values of S_{11}, S_{21}, S_{31}, S_{41} and output phase, validating the design performance. The Butler Matrix with termination load exhibits minimal return losses, with most of the ports showing values below -10 dB, along with acceptable transmission amplitude and isolation performance. In addition, the output phase of terminated the Butler Matrix is found to be consistent within ±10° over a wide frequency band. This study uniquely addresses the integration of RF terminators in the Butler Matrix, mitigating signal degradation, which has not been fully explored in earlier studies. Unlike previous studies, this research provides a detailed analysis of current distribution and experimental validation. The performance analysis confirms the findings and highlights the importance of proper RF termination in high-frequency beamforming systems for reliable, high-performance wireless communication devices.

Acknowledgement

This work was supported by MMU International Matching Grant in collaboration with Telkom University (MMU-TelU) SAP No: MMUE/240035, SAP network No: 4151426, Faculty of Engineering, Multimedia University Cyberjaya and Communication Systems and Network (CSN i-Kohza), UTM KL.

Conflict of Interest

Authors declare that there is no conflict of interest regarding the publication of the paper.

Author Contribution

The authors made contribution to the paper as follows: ***study conception and design:*** Noorlindawaty Md Jizat, Yoshihide Yamada*;* ***data collection:*** Norsiha Zainuddin, Norazah Abdullah*;* ***analysis of results:*** Noorlindawaty Md Jizat, Ayuni Afiqah*;* ***draft manuscript preparation:*** Noorlindawaty Md Jizat; ***supervision and conceptualization*****:** Yoshihide Yamada. *The manuscript's final version has been approved by all authors.*

References

[1] Intan Izafina, I. (2020) *Multibeam array antenna for base station in the fifth-generation mobile communication system/Intan Izafina Idrus*. Universiti Malaya.

[2] Hussain, K. and Oh, I.-Y. (2024) Joint Radar, Communication, and Integration of Beamforming Technology, *Electronics 13* (8), 1531.https://doi.org/10.3390/electronics13081531

[3] Yazdanbakhsh, P. and Solbach, K. (2011) Microstrip Butler matrix design and realization for 7 T MRI, *Magnetic resonance in medicine 66* (1), 270-280.https://doi.org/10.1002/mrm.22777

[4] Song, Y., Wang, H., Liu, W., Xiao, W., Ye, X. and Sun, G. (2024) A review on the mechanism of high repetition rate pulse interference on the RF front-end of GNSS receivers, *Frontiers in Physics 12*, 1447696.https://doi.org/10.3389/fphy.2024.1447696

[5] Jahan, M. I., Faruque, M. R. I., Hossain, M. B., Khandaker, M. U., Elsayed, F., Salman, M. and Osman, H. (2023) Quad-band metamaterial perfect absorber with high shielding effectiveness using double X-shaped ring resonator, *Materials 16* (12), 4405.https://doi.org/10.3390/ma16124405

[6] Chang, L., Zhang, H., Gulliver, T. A. and Lyu, T. (2023) Robust adaptive beamforming for interference suppression based on SNR, *Electronics 12* (21), 4501.https://doi.org/10.3390/electronics12214501

[7] Morgenstern, C. W., Rong, Y., Herschfelt, A., Molnar, A. C., Apsel, A. B., Landon, D. G. and Bliss, D. W. (2023) Analog-domain self-interference cancellation for practical multi-tap full-duplex system: Theory, modeling, and algorithm, *IEEE Journal on Selected Areas in Communications 41* (9), 2796-2807.https://doi.org/10.1109/jsac.2023.3287608

[8] Araujo, R., da Silva, L., Santos, W. and Souza, M. (2023) Cognitive Radio Strategy Combined with MODCOD Technique to Mitigate Interference on Low-Orbit Satellite Downlinks, *Sensors 23* (16), 7234.https://doi.org/10.3390/s23167234

[9] Azari, A., Skrivervik, A. and Aliakbarian, H. (2023) Design methodology for high-performance low-cost microstrip termination load for mmWave applications, *Electronics Letters 59* (22), e13017.https://doi.org/10.1049/ell2.13017

[10] Salih, A. A.-K. and Nangir, M. (2024) Using the Parasitic Element Method to Reduce the Mutual Coupling in the Design of (2x1) MIMO Triple-Band Antenna for 5G Wireless Transmission Application.https://doi.org/10.58346/jowua.2024.i4.018

[11] Bae, B., Kim, J. and Han, K. J. (2020) Numerical verification of dielectric contactor as auxiliary loads for measuring the multi-port network parameter of vertical interconnection array, *IEEE Access 8*, 117997-118004.https://doi.org/10.1109/access.2020.3003231

[12] Wu, T., Jiang, Q., Xie, X., Zhao, H. and Ji, B. (2023) Multi-port admittance model and SISO stability criterion for oscillatory stability analysis of VSC-based AC/DC interconnected renewable systems, *International Journal of Electrical Power & Energy Systems 147*, 108785.https://doi.org/10.1016/j.ijepes.2022.108785

[13] Bunea, A., Neculoiu, D. and Dinescu, M. (2022) Characterization of 3-port SAW diplexers using 2-port VNA measurements. *2022 International Semiconductor Conference (CAS).* IEEE. *https://ieeexplore.ieee.org/document/9934482.*

[14] Raghunandan, K. (2022) Radio Frequency Measurements. *Introduction to Wireless Communications and Networks: A Practical Perspective.* Springer. 405-459.

[15] Han, Y., Liu, Z., Cui, Q. and Qiu, X. (2023) Shielding Effectiveness Evaluation of Enclosure on PCB by Nesting Cavities Test Method, *IEEE Transactions on Instrumentation and Measurement*.https://doi.org/10.1109/tim.2023.3312706

[16] Ushijima, Y., Yukawa, H., Takahashi, T. and Yoneda, N. (2024) K-Band Waveguide Terminator Suitable for Additive Manufacturing Technology and its Applications. *2024 54th European Microwave Conference (EuMC).* IEEE. *https://ieeexplore.ieee.org/document/10732420.*

[17] Laur, V., Maalouf, A., Chevalier, A., Laurent, P. and Zinkiewicz, G. (2022) Ultra-compact K-band microwave terminations. *2022 IEEE Radio and Wireless Symposium (RWS).* IEEE. *https://ieeexplore.ieee.org/document/9719958.*

[18] Lee, S., Lee, Y. and Shin, H. (2021) A 28-GHz switched-beam antenna with integrated Butler matrix and switch for 5G applications, *Sensors 21* (15), 5128.DOI:10.3390/s21155128.

[19] Jeon, M., Seo, Y., Cho, J., Lee, C., Jang, J., Lee, Y., Kwon, H.-W. and Kahng, S. (2021) Investigation on beam alignment of a microstrip-line Butler matrix and an SIW Butler matrix for 5G beamforming antennas through RF-to-RF wireless sensing and 64-QAM tests, *Sensors 21* (20), 6830.https://doi.org/10.3390/s21206830

[20] Chien, Y.-C., Liu, H.-W. and Wu, T.-L. (2022) Reducing the number of measurements of a multiport circuit using covering designs and Turán systems, *IEEE Microwave and Wireless Technology Letters 33* (2), 115-117.https://doi.org/10.1109/lmwc.2022.3215290

[21] Md Jizat, N., Yusoff, Z., Mohd Marzuki, A. S., Zainudin, N. and Yamada, Y. (2022) Insertion Loss and Phase Compensation Using a Circular Slot Via-Hole in a Compact 5G Millimeter Wave (mmWave) Butler Matrix at 28 GHz, *Sensors 22* (5), 1850.https://doi.org/10.3390/s22051850

[22] Bhatta, A., Park, J., Baek, D. and Kim, J.-G. (2023) A Multimode 28 GHz CMOS Fully Differential Beamforming IC for Phased Array Transceivers, *Sensors 23* (13), 6124.https://doi.org/10.3390/s23136124

[23] Wang, B. (2019) Interpolation based wideband beamforming frontends for 5G millimetre wave communication.https://doi.org/10.1109/iscas.2017.8050834

[24] Tan, M. C., Li, M., Abbasi, Q. H. and Imran, M. A. (2020) Design and characterization of T/R module for commercial beamforming applications, *IEEE Access 8*, 130252-130262.https://doi.org/10.1109/access.2020.3009531

[25] Technologies, K. (2024) *How to Measure Return Loss With a Spectrum Analyzer. https://www.keysight.com/used/us/en/knowledge/guides/spectrum-analyzer-buying-guide/how-to-measure-return-loss-with-a-spectrum-analyzer*

[26] Pozar, D. M. (2011) *Microwave engineering.* John wiley & sons.0470631554: 0470631554

[27] Orakwue, S. and Ngah, R. (2019) Switched-beam array antenna at 28 GHz for 5G wireless system based on butler matrix beamforming network, *Nigerian Journal of Technology 38* (2), 484-489.https://doi.org/10.4314/njt.v38i2.27

[28] Peng, W.-H. and Chen, Y.-S. (2025) Beam-Switching Antennas Using a Butler Matrix with a Five-Element Configuration, *Electronics (2079-9292) 14* (5).https://doi.org/10.3390/electronics14050959

[29] Lee, C. M., Chi, J. G., Yook, J. M. and Kim, Y. J. (2022) A compact design of a wideband millimeter-wave Butler matrix using integrated passive device technology, *Microwave and Optical Technology Letters 64* (11), 1888-1894.https://doi.org/10.1002/mop.33392 .